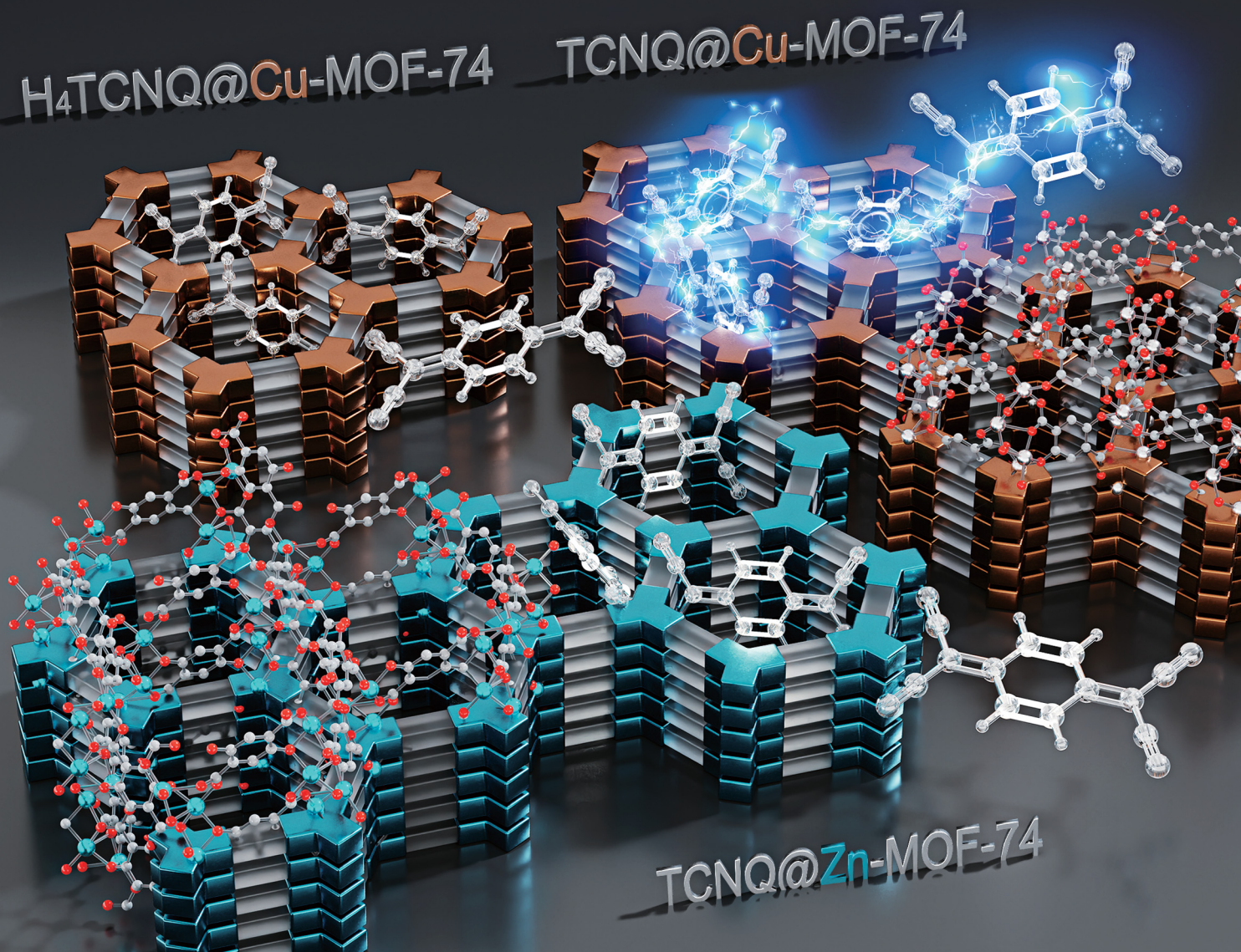


Journal of Materials Chemistry C

Materials for optical, magnetic and electronic devices

rsc.li/materials-c



ISSN 2050-7526

COMMUNICATION

Monica C. So *et al.*

From insulator to semiconductor: effect of host-guest interactions on charge transport in M-MOF-74 metal-organic frameworks

Cite this: *J. Mater. Chem. C*,
2024, 12, 2699Received 13th November 2023,
Accepted 8th January 2024

DOI: 10.1039/d3tc04155g

rsc.li/materials-c

From insulator to semiconductor: effect of host–guest interactions on charge transport in M-MOF-74 metal–organic frameworks†

Sydney M. Angel,^a Nicholas S. Barnett,^{ab} A. Alec Talin,^c Michael E. Foster,^c
Vitalie Stavila,^{ib} Mark D. Allendorf^{ib} and Monica C. So^{ib}*^a

Here, we report an air-free approach to infiltrate isostructural metal–organic frameworks (MOFs), M-MOF-74 (M = Cu, Mn, Zn, Mg), with conjugated acceptor 7,7,8,8-tetracyanoquinodimethane (TCNQ). The TCNQ@M-MOF-74 compounds exhibit a striking correlation between their bulk conductivities and the open *d* shell variants (Cu, Mn), arising from TCNQ p-doping of the MOFs. Importantly, conjugation of the guest molecule is a prerequisite for inducing electrical conductivity in these systems.

Combining the tunability and porosity of metal–organic frameworks (MOFs) with electronic (semi-)conductivity has driven the development of electronics, such as chemical sensors,^{1–3} photovoltaics,^{4–7} low-*k* dielectrics,^{8,9} and non-volatile memory elements.¹⁰ However, most existing MOFs are insulators due to the poor overlap between π orbitals of the organic linkers and *d* orbitals of the metal ions, suppressing charge transfer. By judiciously selecting metal ions with high-energy valence electrons and organic linkers that form coordination bonds with increased orbital delocalization between metal and linker, conductive MOFs have been realized.^{6,11–14}

A paradigm-shifting alternative approach, which some of our team explored, successfully rendered the insulating Cu₃(btc)₂ MOF into an electrically conductive one by introducing a conjugated and redox-active guest molecule, 7,7,8,8-tetracyanoquinodimethane (TCNQ).¹⁵ Since then, we also uncovered that the preferential ordering of the TCNQ molecules along the (111) lattice plane within HKUST-1 and the TCNQ bridging coordination motif to two adjacent copper paddlewheels facilitate conductivity.¹⁶ Recently, others adapted this infiltration strategy for M-MOF-74 (M = Co,¹ Mn¹⁷) with

densely packed open metal sites (OMS)^{18–26} for effective host–guest interaction. To date, none have elucidated the nature of the host–guest complex or proposed conductivity mechanisms in the TCNQ@M-MOF-74 system. In general, the interaction between the guest and the host has been characterized as ‘redox doping’,^{27,28} resulting in charge transfer and the formation of mobile charge carriers in the MOF conduction or valence bands and thus increased electrical conductivity.^{29,30} However, these previous studies failed to address additional fundamental questions, such as: to what extent do open *d* shells of metal ions in M-MOF-74 influence charge transfer? What role does conjugation play in TCNQ in influencing electrical conductivity? How does oxygen affect the stability of TCNQ? Through what charge transport mechanism does TCNQ induce MOF conductivity?

These unanswered questions motivated us to closely scrutinize the nature of TCNQ@M-MOF-74 interactions that contribute to bulk conductivity. Recently, Bláha and colleagues confirmed charge transfer between TCNQ and Mn-MOF-74 by diagnostic Raman stretches, but their approach resulted in oxidized TCNQ.¹⁷ Samples were further handled under ambient conditions, contaminating the host–guest system with oxygen. Our work expands upon their integral efforts, applying an air-free TCNQ infiltration approach into isostructural M-MOF-74, where M is divalent Mg, Mn, Cu, and Zn. Through rigorous exclusion of oxygen, our inert infiltration method yields no oxidized TCNQ. The coordination of TCNQ to the OMS of M-MOF-74 was confirmed by spectroscopy. Strikingly, we reveal that M-MOF-74 with open *d* shells and conjugated guest molecules are critical in forming charge transport networks, which are supported by temperature-dependent electrical conductivity measurements and density functional theory (DFT) calculations. Importantly, we propose a plausible mechanism to rationalize TCNQ binding to OMS of M-MOF-74 framework to form a continuous network. Together, the experimental and theoretical results in this work shows that TCNQ p-dopes the M-MOF-74 (M = Cu, Mn) hosts, facilitating through-bond charge transport *via* conjugated TCNQ guests.

^a Department of Chemistry and Biochemistry, California State University, Chico, Chico, CA 95973, USA. E-mail: mso@csuchico.edu

^b Department of Physics, University of Illinois, Chicago, Chicago, IL, USA

^c Sandia National Laboratories, Livermore, CA 94551, USA

† Electronic supplementary information (ESI) available: Procedures, materials, and instrumentation; characterization (PXRD, SEM, Raman, EA, UV, DRS, conductivity). See DOI: <https://doi.org/10.1039/d3tc04155g>

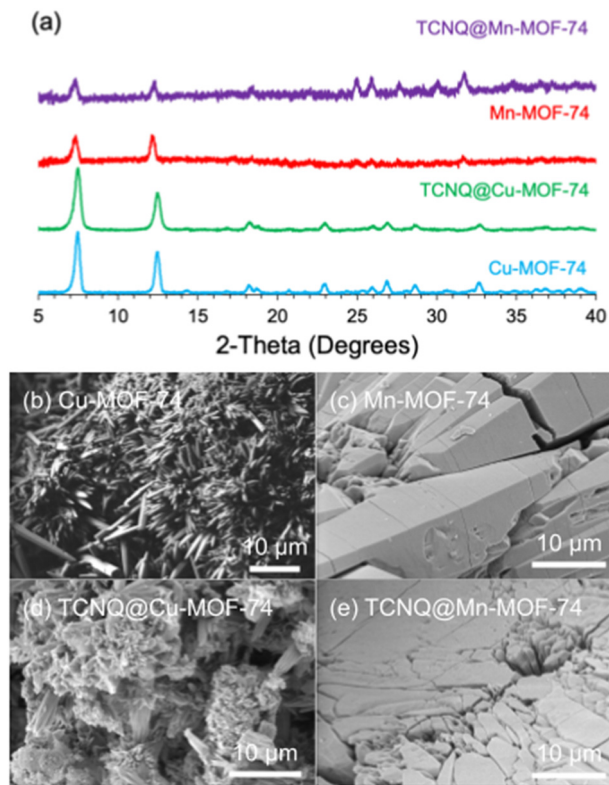


Fig. 1 (a) PXRD of M-MOF-74 and TCNQ@M-MOF for M = Cu, Mn and SEM of (b) Cu-MOF-74, (c) Mn-MOF-74, (d) TCNQ@Cu-MOF-74, and (e) TCNQ@Mn-MOF-74.

The powder X-ray diffraction (PXRD) scans confirm the identity of the M-MOF-74 (M = Cu, Mn, Zn, Mg) powders. PXRDs indicate M-MOF-74 are indeed isostructural, differing only differ by the metal ion (Fig. 1a and Fig. S2, ESI[†]). After TCNQ infiltration (Fig. 1b–e and Fig. S2, ESI[†]), the MOFs not only remained crystalline but retained the same rough, porous morphology with some polycrystallinity. The presence of TCNQ in the MOFs was also confirmed by elemental analysis (Table S1, ESI[†]). There are 2 TCNQs per cell of Cu-MOF-74 (1 TCNQ per 6 copper ions) and 4 TCNQs per cell of Mn-MOF-74 (2 TCNQ per 6 manganese ions). Importantly, there is no evidence of metal-containing TCNQ nanowires in the SEM data; these may form when TCNQ and M(II) are being reduced to TCNQ^{•−} and M(I) by oxidation.¹⁶

To track the coordination of TCNQ to the OMS, Raman spectra were collected for TCNQ@M-MOF-74 (M = Cu, Mn). The frequencies of C=C and C≡N stretching modes of the TCNQ change depending on the degree of charge transfer in both MOF analogues. The 114 cm^{−1} mode shift of the C-CN wing stretch of TCNQ from 1462 to 1348 cm^{−1} indicate that TCNQ interacts with the OMS on the Cu²⁺ ions in Cu-MOF-74 (Fig. 2a). The same shift occurs when TCNQ interacts with the OMS on the Mn²⁺ ions in Mn-MOF-74 (Fig. 2b). A red shift of 19 cm^{−1} for the C=C wing stretching mode suggests a partial charge transfer of ~0.3 e[−] between the framework and TCNQ.³¹ The C≡N stretch at 2230 cm^{−1} indicates coordination of the TCNQ

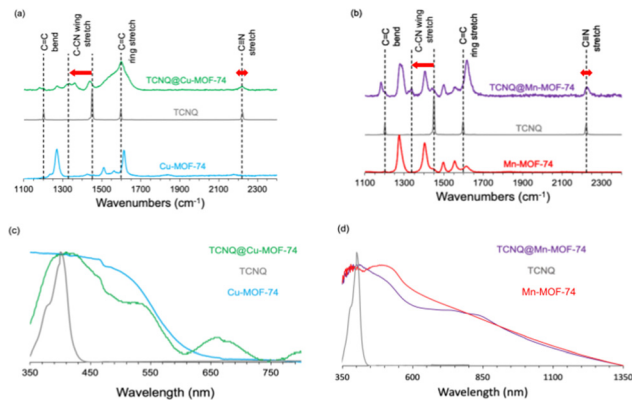


Fig. 2 Raman spectra of (a) Cu-MOF-74 and (b) Mn-MOF-74 before and after TCNQ infiltration. (c) Transmission UV-Vis absorbance spectra of Cu-MOF-74 and (d) diffuse reflectance spectra of Mn-MOF-74 before and after TCNQ infiltration.

molecule to the metal ion for Cu-MOF-74 and Mn-MOF-74 (Fig. 2a and b).

The C≡N stretch of TCNQ is also substantially broadened by adsorption for both analogues. Strikingly, the aforementioned signals are absent from Mg-MOF-74 and Zn-MOF-74 (Fig. S4a and b, ESI[†]), indicating the absence of TCNQ coordination.

With the TCNQ@M-MOF-74 (M = Cu, Mn) in hand, we performed UV-vis absorption and diffuse reflectance spectroscopies to evaluate intermolecular charge transfer. After TCNQ infiltration of Cu-MOF-74 and Mn-MOF-74, there is no band corresponding to the oxidation product of TCNQ^{2−}, dicyano-*p*-toluoyl cyanide, at 480 nm, as expected by eliminating oxygen during infiltration of the M-MOF-74 samples with TCNQ in the glovebox. Importantly, unlike the un-infiltrated MOF-74 samples, new lower energy absorption peaks appear at 660 and 800 nm (green, Fig. 2c) and 850 nm (purple, Fig. 2d), respectively. The strong 660 nm peak of TCNQ@Cu-MOF-74 is attributed to TCNQ^{2−} formed by disproportionation of TCNQ^{•−} dimer, suggesting a salt of [TCNQ]^{2−}[Cu-MOF-74]²⁺ formed.¹ The weaker absorption band at 800 nm for TCNQ@Cu-MOF-74 originates from the TCNQ^{•−} monomer.²⁷ The 850 nm peak in TCNQ@Mn-MOF-74 represents donor–acceptor charge transfer between the Mn-MOF-74 and confined TCNQ guests.¹² We also observe the optical band gaps decrease from 3.08 eV to 1.88 eV and from 2.48 eV to 1.46 eV, consistent with the formation of more conducting TCNQ@Cu-MOF-74 and TCNQ@Mn-MOF-74, respectively. These band gaps are comparable to those previously reported for TCNQ@Co-MOF-74 (1.5 eV)¹ and TCNQ@Cu₃(btc)₂ (1.76 eV).¹⁵

To determine the electronic conductivity, electrical transport measurements were performed on MOF pellets using a two-point probe geometry with large area electrodes to decrease the contact resistance. We used temperature-dependent measurements to extract the activation energy for electronic transport. Conductivity data gathered for all MOF pellets were at temperatures well below the MOF-74 thermal decomposition of 593 K.¹ We observe no detectable conductivity for TCNQ@M-MOF-74

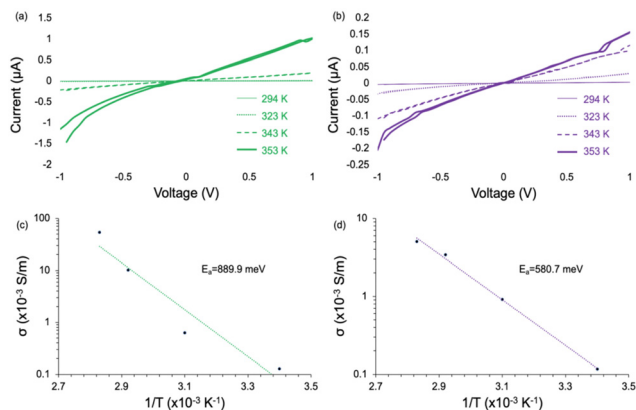


Fig. 3 IV curves for (a) TCNQ@Cu-MOF-74 and (b) TCNQ@Mn-MOF-74, along with corresponding Arrhenius plots for (c) TCNQ@Cu-MOF-74 and (d) TCNQ@Mn-MOF-74.

(M = Mg, Zn) (Fig. S5, ESI[†]) as a function of increasing temperature, which is consistent with the lack of TCNQ coordination in these two variants. In contrast, as we increased the temperature from 294 K to 353 K for TCNQ@Cu-MOF-74 and TCNQ@Mn-MOF-74, their conductivity increased up to $5.40 \times 10^{-2} \text{ S m}^{-1}$ and $5.02 \times 10^{-3} \text{ S m}^{-1}$ with activation energies of 889.9 meV and 580.7 meV, respectively (Fig. 3). These values are similar to those previously reported for TCNQ@Co-MOF-74.¹ Notably, the nonlinear activation energy of TCNQ@Cu-MOF-74 is attributed to the electron–electron Coulombic interactions of copper which varies by temperature. This interaction reduces the density of states near the Fermi level at lower temperatures ($T < 323 \text{ K}$ in Fig. 3c), thus increasing activation energy.³² At $T > 323 \text{ K}$, lattice vibrations intensify, weakening electron binding in the outer layer of the atomic nucleus. Electrons likely move away from the nucleus, thus decreasing activation energy.³³

To develop a deeper understanding of how TCNQ increases the electronic conductivity of Cu-MOF-74 and Mn-MOF-74, we performed DFT calculations. As illustrated in Fig. 4a, the calculations indicate that TCNQ covalently binds to the OMS of the MOFs and that TCNQ molecules may form a new continuous network through the unit cell. Our calculations further show that the LUMO of TCNQ appears near the valence band of the MOFs (Fig. 4b). For TCNQ@Cu-MOF-74, the LUMO of TCNQ slightly overlaps with the valence band of the MOF, as indicated by the blue/green shaded regions in Fig. 4b. The resulting greater degree of overlap is consistent with the larger conductivity observed for the Cu variant compared to the Mn analogue (Fig. 4c). Electron transfer from the MOFs to TCNQ is also predicted by Bader charge analysis (Table S2, ESI[†]), suggesting that TCNQ p-dopes the MOFs in both analogues.

To further probe the effects of guest molecule on the formation of molecular pathways, we infiltrated the Cu and Mn versions of M-MOF-74 with the fully hydrogenated analogue of TCNQ, (cyclohexane-1,4-diylidene)dimalononitrile (H_4TCNQ). Elemental analysis indicates that the loading of H_4TCNQ is similar to that of TCNQ (*i.e.* 2 H_4TCNQ molecules

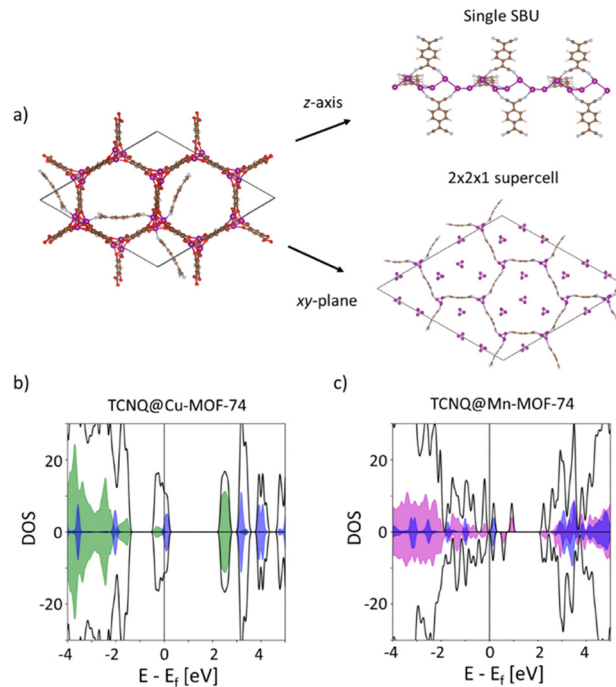


Fig. 4 (a) Possible configuration predicted by DFT calculations of how TCNQ may provide continuous molecular networks through the M-MOF-74 unit cell. On the right, only the TCNQ and metal atoms are shown to illustrate the new channels in the z- (top) and xy-directions (bottom). In the HSE06 total and partial density of states for (b) TCNQ@Cu-MOF-74 and (c) TCNQ@Mn-MOF-74, the blue curve is the sum of states on the TCNQ molecule, and green/magenta curves are the Cu/Mn states, respectively.

per Cu-MOF-74 cell and 4 TCNQ molecules per Mn-MOF-74 cell). Although Raman suggests H_4TCNQ coordination to the OMS with a C-CN wing stretch shift and $\text{C}\equiv\text{N}$ stretch broadening (Fig. S4c and d, ESI[†]), we observed that $\text{H}_4\text{TCNQ}@M\text{-MOF-74}$ (M = Cu, Mn) exhibit no detectable conductivity (Fig. S6a and b, ESI[†]). The same applies to the magnesium and zinc variants (Fig. S6c and d, ESI[†]). The crystals remained insulating, since the H_4TCNQ lacks a conjugated π electron network. Therefore, the presence of conjugation in the guest molecule is critical in completing the molecular network necessary for inducing conductivity in TCNQ@M-MOF-74, as was observed for TCNQ@Cu₃(BTC)₂.¹⁵

In summary, we employed an air-free approach to infiltrate a series of isostructural M-MOF-74 (M = Cu, Mn, Zn, Mg) with TCNQ. This strategy produced no oxidized TCNQ²⁻ by-product, unlike ambient infiltration strategy performed in previous studies. Infiltration of TCNQ into open *d* shell variants Cu-MOF-74 and Mn-MOF-74 yielded electrically conductive materials. Interestingly, the introduction of H_4TCNQ to the copper and manganese M-MOF-74 did not improve the conductivity, indicating the need for a conjugated π -network in the guest molecules to facilitate proper band alignment and thus charge transport. To our knowledge, this is the first work with computational evidence proposing an important structure–property relationship—binding of TCNQ to the OMS forms new molecular pathways and p-dopes the MOF-74 framework. Since most

current conductive materials have limited chemical tunability, this work is an important step towards understanding how alternative charge transport pathways may help access conductive behavior in insulating inorganic parent materials. To guide future experimental efforts, computational analysis can determine what modifications make certain MOFs hold more metallic properties^{29,30,34} or predict which MOFs will have lower bandgaps.³⁵ By fundamentally understanding host–guest interactions, we can unlock the potential to transforming insulating materials into novel nanoporous conductive MOFs for electronic devices.^{4,5,15,36,37}

S. M. A., N. S. B., and M. C. S. carried out all synthesis and characterization. M. C. S. interpreted PXRD, SEM, Raman, DRS, UV, and conductivity data. M. E. F. performed and interpreted DFT calculations. V. N. S. collected and interpreted E. A. data. M. C. S. directed the project, as well as wrote and revised the manuscript with assistance from S. M. A. and N. S. B. A. A. T., V. N. S., and M. D. A. revised and polished the manuscript, as well as helped supervised the project. V. N. S. conceived the original idea.

M. C. S. acknowledges support from the National Science Foundation (CMMI-1920332, DMR-2137915), Camille and Henry Dreyfus Foundation (TH-23-035), and U.S. Department of Energy, Office of Science, Offices of Basic Energy Sciences and Electricity under contract DE-SC0024581. N. S. B. thanks CSU Chico's Lantis University Foundation. M. C. S. and S. M. A. are also grateful for support by the U.S. Department of Energy, Office of Science, Office of Workforce Development for Teachers and Scientists (WDTS), under the Visiting Faculty Program (VFP). Work at the Molecular Foundry was supported by the Office of Science, Office of Basic Energy Sciences, of the U.S. Department of Energy under Contract No. DE-AC02-05CH11231. Funding for this project was also provided by the Sandia Laboratory Directed Research and Development (LDRD) Program. AAT was supported by the Center for Reconfigurable Electronic Materials Inspired by Nonlinear Neuron Dynamics (reMIND), an Energy Frontier Research Center funded by the U.S. Department of Energy, Office of Science, Basic Energy Sciences. Sandia National Laboratories is a multi-mission laboratory managed and operated by National Technology and Engineering Solutions of Sandia, LLC, a wholly owned subsidiary of Honeywell International, Inc., for the U.S. Department of Energy's National Nuclear Security Administration under contract DE-NA-0003525. This paper describes objective technical results and analysis. Any subjective views or opinions that might be expressed in the paper do not necessarily represent the views of the U.S. Department of Energy or the U.S. Government. We would like to finally thank James J. Calvo and Annabelle Benin for assistance with sample preparation and Ryan Nishimoto for assistance with SEM measurements.

Conflicts of interest

There are no conflicts to declare.

Notes and references

- H. Shiozawa, B. C. Bayer, H. Peterlik, J. C. Meyer, W. Lang and T. Pichler, Doping of Metal–Organic Frameworks towards Resistive Sensing, *Sci. Rep.*, 2017, 7(1), 2439, DOI: [10.1038/s41598-017-02618-y](https://doi.org/10.1038/s41598-017-02618-y).
- I. Stassen, N. Burtch, A. Talin, P. Falcaro, M. Allendorf and R. Ameloot, An Updated Roadmap for the Integration of Metal–Organic Frameworks with Electronic Devices and Chemical Sensors, *Chem. Soc. Rev.*, 2017, 46(11), 3185–3241, DOI: [10.1039/C7CS00122C](https://doi.org/10.1039/C7CS00122C).
- M. Campbell and M. Dincă, Metal–Organic Frameworks as Active Materials in Electronic Sensor Devices, *Sensors*, 2017, 17(5), 1108, DOI: [10.3390/s17051108](https://doi.org/10.3390/s17051108).
- M. C. So, S. Jin, H.-J. Son, G. P. Wiederrecht, O. K. Farha and J. T. Hupp, Layer-by-Layer Fabrication of Oriented Porous Thin Films Based on Porphyrin-Containing Metal–Organic Frameworks, *J. Am. Chem. Soc.*, 2013, 135(42), 15698–15701, DOI: [10.1021/ja4078705](https://doi.org/10.1021/ja4078705).
- H. J. Park, M. C. So, D. Gosztola, G. P. Wiederrecht, J. D. Emery, A. B. F. Martinson, S. Er, C. E. Wilmer, N. A. Vermeulen, A. Aspuru-Guzik, J. F. Stoddart, O. K. Farha and J. T. Hupp, Layer-by-Layer Assembled Films of Perylene Diimide- and Squaraine-Containing Metal–Organic Framework-like Materials: Solar Energy Capture and Directional Energy Transfer, *ACS Appl. Mater. Interfaces*, 2016, 8(38), 24983–24988, DOI: [10.1021/acsami.6b03307](https://doi.org/10.1021/acsami.6b03307).
- S. Yoon, A. A. Talin, V. Stavila, A. M. Mroz, T. D. Bennett, Y. He, D. A. Keen, C. H. Hendon, M. D. Allendorf and M. C. So, From N- to p-Type Material: Effect of Metal Ion on Charge Transport in Metal–Organic Materials, *ACS Appl. Mater. Interfaces*, 2021, 13(44), 52055–52062, DOI: [10.1021/acsami.1c09130](https://doi.org/10.1021/acsami.1c09130).
- J. J. Calvo, S. M. Angel and M. C. So, Charge Transport in Metal–Organic Frameworks for Electronics Applications, *APL Mater.*, 2020, 8(5), 050901, DOI: [10.1063/1.5143590](https://doi.org/10.1063/1.5143590).
- M. D. Allendorf, A. Schwartzberg, V. Stavila and A. A. Talin, A Roadmap to Implementing Metal–Organic Frameworks in Electronic Devices: Challenges and Critical Directions, *Chem. – Eur. J.*, 2011, 17(41), 11372–11388, DOI: [10.1002/chem.201101595](https://doi.org/10.1002/chem.201101595).
- K. Zagorodniy, G. Seifert and H. Hermann, Metal–Organic Frameworks as Promising Candidates for Future Ultralow-k Dielectrics, *Appl. Phys. Lett.*, 2010, 97(25), 251905, DOI: [10.1063/1.3529461](https://doi.org/10.1063/1.3529461).
- S. M. Yoon, S. C. Warren and B. A. Grzybowski, Storage of Electrical Information in Metal–Organic-Framework Memristors, *Angew. Chem., Int. Ed.*, 2014, 53(17), 4437–4441, DOI: [10.1002/anie.201309642](https://doi.org/10.1002/anie.201309642).
- D. Sheberla, L. Sun, M. A. Blood-Forsythe, S. Er, C. R. Wade, C. K. Brozek, A. Aspuru-Guzik and M. Dincă, High Electrical Conductivity in Ni₃(2,3,6,7,10,11-Hexamino-triphenylene)₂, a Semiconducting Metal–Organic Graphene Analogue, *J. Am. Chem. Soc.*, 2014, 136(25), 8859–8862, DOI: [10.1021/ja502765n](https://doi.org/10.1021/ja502765n).

- 12 S. Yamamoto, J. Pirillo, Y. Hijikata, Z. Zhang and K. Awaga, Nanopore-Induced Host–Guest Charge Transfer Phenomena in a Metal–Organic Framework, *Chem. Sci.*, 2018, **9**(13), 3282–3289, DOI: [10.1039/C7SC05390H](https://doi.org/10.1039/C7SC05390H).
- 13 A. J. Clough, J. M. Skelton, C. A. Downes, A. A. de la Rosa, J. W. Yoo, A. Walsh, B. C. Melot and S. C. Marinescu, Metallic Conductivity in a Two-Dimensional Cobalt Dithiolenic Metal–Organic Framework, *J. Am. Chem. Soc.*, 2017, **139**(31), 10863–10867, DOI: [10.1021/jacs.7b05742](https://doi.org/10.1021/jacs.7b05742).
- 14 L. Sun, C. H. Hendon, M. A. Minier, A. Walsh and M. Dincă, Million-Fold Electrical Conductivity Enhancement in Fe₂ (DEBDC) versus Mn₂ (DEBDC) (E = S, O), *J. Am. Chem. Soc.*, 2015, **137**(19), 6164–6167, DOI: [10.1021/jacs.5b02897](https://doi.org/10.1021/jacs.5b02897).
- 15 A. A. Talin, A. Centrone, A. C. Ford, M. E. Foster, V. Stavila, P. Haney, R. A. Kinney, V. Szalai, F. El Gabaly, H. P. Yoon, F. Léonard and M. D. Allendorf, Tunable Electrical Conductivity in Metal–Organic Framework Thin-Film Devices, *Science*, 2014, **343**(6166), 66–69, DOI: [10.1126/science.1246738](https://doi.org/10.1126/science.1246738).
- 16 C. Schneider, D. Ukaj, R. Koerver, A. A. Talin, G. Kieslich, S. P. Pujari, H. Zuilhof, J. Janek, M. D. Allendorf and R. A. Fischer, High Electrical Conductivity and High Porosity in a Guest@MOF Material: Evidence of TCNQ Ordering within Cu₃ BTC₂ Micropores, *Chem. Sci.*, 2018, **9**(37), 7405–7412, DOI: [10.1039/C8SC02471E](https://doi.org/10.1039/C8SC02471E).
- 17 M. Bláha, V. Valeš, Z. Bastl, M. Kalbáč and H. Shiozawa, Host–Guest Interactions in Metal–Organic Frameworks Doped with Acceptor Molecules as Revealed by Resonance Raman Spectroscopy, *J. Phys. Chem. C*, 2020, **124**(44), 24245–24250, DOI: [10.1021/acs.jpcc.0c07473](https://doi.org/10.1021/acs.jpcc.0c07473).
- 18 W. Zhou, H. Wu and T. Yildirim, Enhanced H₂ Adsorption in Isostructural Metal–Organic Frameworks with Open Metal Sites: Strong Dependence of the Binding Strength on Metal Ions, *J. Am. Chem. Soc.*, 2008, **130**(46), 15268–15269, DOI: [10.1021/ja807023q](https://doi.org/10.1021/ja807023q).
- 19 L. Valenzano, B. Civalleri, S. Chavan, G. T. Palomino, C. O. Areán and S. Bordiga, Computational and Experimental Studies on the Adsorption of CO, N₂, and CO₂ on Mg-MOF-74, *J. Phys. Chem. C*, 2010, **114**(25), 11185–11191, DOI: [10.1021/jp102574f](https://doi.org/10.1021/jp102574f).
- 20 R. Poloni, K. Lee, R. F. Berger, B. Smit and J. B. Neaton, Understanding Trends in CO₂ Adsorption in Metal–Organic Frameworks with Open-Metal Sites, *J. Phys. Chem. Lett.*, 2014, **5**(5), 861–865, DOI: [10.1021/jz500202x](https://doi.org/10.1021/jz500202x).
- 21 K. Tan, S. Zuluaga, Q. Gong, P. Canepa, H. Wang, J. Li, Y. J. Chabal and T. Thonhauser, Water Reaction Mechanism in Metal Organic Frameworks with Coordinatively Unsaturated Metal Ions: MOF-74, *Chem. Mater.*, 2014, **26**(23), 6886–6895, DOI: [10.1021/cm5038183](https://doi.org/10.1021/cm5038183).
- 22 E. Haldoupis, J. Borycz, H. Shi, K. D. Vogiatzis, P. Bai, W. L. Queen, L. Gagliardi and J. I. Siepmann, Ab Initio Derived Force Fields for Predicting CO₂ Adsorption and Accessibility of Metal Sites in the Metal–Organic Frameworks M-MOF-74 (M = Mn, Co, Ni, Cu), *J. Phys. Chem. C*, 2015, **119**(28), 16058–16071, DOI: [10.1021/acs.jpcc.5b03700](https://doi.org/10.1021/acs.jpcc.5b03700).
- 23 K. Lee, J. D. Howe, L.-C. Lin, B. Smit and J. B. Neaton, Small-Molecule Adsorption in Open-Site Metal–Organic Frameworks: A Systematic Density Functional Theory Study for Rational Design, *Chem. Mater.*, 2015, **27**(3), 668–678, DOI: [10.1021/cm502760q](https://doi.org/10.1021/cm502760q).
- 24 H. Jiang, Q. Wang, H. Wang, Y. Chen and M. Zhang, MOF-74 as an Efficient Catalyst for the Low-Temperature Selective Catalytic Reduction of NO_x with NH₃, *ACS Appl. Mater. Interfaces*, 2016, **8**(40), 26817–26826, DOI: [10.1021/acsami.6b08851](https://doi.org/10.1021/acsami.6b08851).
- 25 I. Strauss, A. Mundstock, D. Hinrichs, R. Himstedt, A. Knebel, C. Reinhardt, D. Dorfs and J. Caro, The Interaction of Guest Molecules with Co-MOF-74: A Vis/NIR and Raman Approach, *Angew. Chem., Int. Ed.*, 2018, **57**(25), 7434–7439, DOI: [10.1002/anie.201801966](https://doi.org/10.1002/anie.201801966).
- 26 I. Strauss, A. Mundstock, M. Treger, K. Lange, S. Hwang, C. Chmelik, P. Rusch, N. C. Bigall, T. Pichler, H. Shiozawa and J. Caro, Metal–Organic Framework Co-MOF-74-Based Host–Guest Composites for Resistive Gas Sensing, *ACS Appl. Mater. Interfaces*, 2019, **11**(15), 14175–14181, DOI: [10.1021/acsami.8b22002](https://doi.org/10.1021/acsami.8b22002).
- 27 R. H. Boyd and W. D. Phillips, Solution Dimerization of the Tetracyanoquinodimethane Ion Radical, *J. Chem. Phys.*, 1965, **43**(9), 2927–2929, DOI: [10.1063/1.1697251](https://doi.org/10.1063/1.1697251).
- 28 L. R. Melby, R. J. Harder, W. R. Hertler, W. Mahler, R. E. Benson and W. E. Mochel, Substituted Quinodimethanes. II. Anion-Radical Derivatives and Complexes of 7,7,8,8-Tetracyanoquinodimethane, *J. Am. Chem. Soc.*, 1962, **84**(17), 3374–3387, DOI: [10.1021/ja00876a029](https://doi.org/10.1021/ja00876a029).
- 29 M. E. Foster, K. Sohlberg, C. D. Spataru and M. D. Allendorf, Proposed Modification of the Graphene Analogue Ni₃ (HITP)₂ To Yield a Semiconducting Material, *J. Phys. Chem. C*, 2016, **120**(27), 15001–15008, DOI: [10.1021/acs.jpcc.6b05746](https://doi.org/10.1021/acs.jpcc.6b05746).
- 30 M. E. Foster, K. Sohlberg, M. D. Allendorf and A. A. Talin, Unraveling the Semiconducting/Metallic Discrepancy in Ni₃ (HITP)₂, *J. Phys. Chem. Lett.*, 2018, **9**(3), 481–486, DOI: [10.1021/acs.jpclett.7b03140](https://doi.org/10.1021/acs.jpclett.7b03140).
- 31 S. Matsuzaki, R. Kuwata and K. Toyoda, Raman Spectra of Conducting TCNQ Salts; Estimation of the Degree of Charge Transfer from Vibrational Frequencies, *Solid State Commun.*, 1980, **33**(4), 403–405, DOI: [10.1016/0038-1098\(80\)90429-9](https://doi.org/10.1016/0038-1098(80)90429-9).
- 32 M. Pollak, Effect of carrier-carrier interactions on some transport properties in disordered semiconductors, *Discuss. Faraday Soc.*, 1970, **50**, 13–19.
- 33 V. Ambegaokar, B. I. Halperin and J. S. Langer, Hopping conductivity in disordered systems, *Phys. Rev. B: Solid State*, 1971, **4**(8), 2612–2620.
- 34 M. Kriebel, M. Hennemann, F. R. Beierlein, D. D. Medina, T. Bein and T. Clark, Propagation of Holes and Electrons in Metal–Organic Frameworks, *J. Chem. Inf. Model.*, 2019, **59**(12), 5057–5064, DOI: [10.1021/acs.jcim.9b00461](https://doi.org/10.1021/acs.jcim.9b00461).
- 35 A. S. Rosen, S. M. Iyer, D. Ray, Z. Yao, A. Aspuru-Guzik, L. Gagliardi, J. M. Notestein and R. Q. Snurr, Machine Learning the Quantum-Chemical Properties of Metal–Organic Frameworks for Accelerated Materials Discovery, *Matter*, 2021, **4**(5), 1578–1597, DOI: [10.1016/j.matt.2021.02.015](https://doi.org/10.1016/j.matt.2021.02.015).

- 36 T. Ohata, A. Nomoto, T. Watanabe, I. Hirose, T. Makita, J. Takeya and R. Makiura, Uniaxially Oriented Electrically Conductive Metal–Organic Framework Nanosheets Assembled at Air/Liquid Interfaces, *ACS Appl. Mater. Interfaces*, 2021, **13**(45), 54570–54578, DOI: [10.1021/acsami.1c16180](https://doi.org/10.1021/acsami.1c16180).
- 37 P. I. Scheurle, A. Mähringer, A. Biewald, A. Hartschuh, T. Bein and D. D. Medina, MOF-74(M) Films Obtained through Vapor-Assisted Conversion—Impact on Crystal Orientation and Optical Properties, *Chem. Mater.*, 2021, **33**(15), 5896–5904, DOI: [10.1021/acs.chemmater.1c00743](https://doi.org/10.1021/acs.chemmater.1c00743).